

Morphology Determination of Novel Polysulfone–Polyamide Block Copolymers Using Element Spectroscopic Imaging in the Transmission Electron Microscopy

Alexander E. Ribbe,[†] Masaki Hayashi,[†] Martin Weber,[‡] and Takeji Hashimoto^{†,*}

Department of Polymer Chemistry, Graduate School of Engineering, Kyoto University, Kyoto 606-8501, Japan, and BASF AG, Polymer Research Laboratory, 67056 Ludwigshafen, Germany

Received April 8, 1999

Revised Manuscript Received December 6, 1999

Introduction. Although the element spectroscopic imaging technique (ESI) (sometimes also called element specific imaging or energy filtered transmission electron microscopy EFTEM) has been available now for more than 10 years, this method is still not very intensively used by the polymer research community. The method, which can be considered as an extension of the classic electron energy loss spectroscopy in two dimensions, allows the investigation of the morphology of polymer blends,¹ block copolymers,² or polymer composites³ in a less-destructive way. The less-destructive way means, in this case, that compared to the conventional transmission electron microscopy (CTEM), no staining, which influences the morphology in an unpredictable way, is necessary to obtain a phase contrast. The extent of damage due to the electron beam, however, is the same for both ESI and CTEM. The technique relies on the energy loss of inelastically scattered electrons, which is specific for every electron shell of an element. If one of the phases of a multiphase system contains specifically one kind of atom, which is not contained in another phase of the system, the structure can be visualized by determination of a so called element mapping. The established way to obtain such an element mapping is the so called three-window method: In order to execute an element mapping, a background image is calculated from two background images in front of the element edge of our interest, and this background image which is extrapolated to the postedge image is now subtracted from the postedge image to obtain the element mapping. Further details would exceed the scope of this paper and can be found in the literature.⁴

Compared to block copolymers made by living anionic polymerization, which have a very narrow, sometimes almost monodisperse, molecular weight distribution, block copolymers made by polycondensation have a wide polydispersity. Usually almost monodisperse block copolymers show a more or less regular spherical, cylindrical, lamellar, or bicontinuous microdomain structure, depending on the molecular weight ratio of the two blocks,⁵ as a consequence of the microphase separation. Polysulfone-*block*-polyamide (PSU-PA) block copolymers, to be discussed in this paper, which are prepared by polycondensation, show a large polydispersity, and therefore a not very well ordered microdomain structure can be expected. In contrast to other block copolymers, which can sometimes easily be stained by osmium

tetraoxide or ruthenium tetraoxide, the staining of the PSU-PA block copolymer investigated here, coded PSU-PAI, by osmium or ruthenium tetraoxide leads to unsatisfactory results. Since element distribution images only rely on inelastically scattered electrons by a specifically contained element, the phase structure determination of the PSU-PA block copolymer is possible by determination of a spatial distribution of sulfur contained only in the PSU phase and of nitrogen contained only in the PA phase. Our aim is not to prove that the ESI method is useful and works well for our system by comparing it to conventional TEM images and scattering profiles, but rather to give insight into the morphology of a novel PSU-PA block copolymer for which the standard staining methods do not work and to show that the ESI method is the only applicable real-space method. Furthermore the small-angle X-ray scattering (SAXS) profiles showed only monotonous profiles having a very broad scattering maximum or shoulder and hence are not providing specific information regarding the real-space morphology.

Experimental Section. Synthesis and Characterization. In a 2 L four-neck flask equipped with a stirrer, a reflux condenser, and a nitrogen inlet, 100 g of an anhydride terminated polysulfone (PSU-PhA) was dissolved in 500 mL of dry *N*-methylpyrrolidone (NMP) under N₂ atmosphere. To this solution, a solution of 100 g of an amorphous polyamide (PAI) dissolved in 500 mL of dry NMP was added over a period of 30 min. After further stirring for 30 min the homogeneous solution was heated to 195 °C for 6 h. Afterward the reaction product was isolated by precipitation in 6 L of water. After filtration the product was dried at 130 °C under vacuum for 24 h.

In order to separate the block copolymer from unreacted homopolymer, the material was extracted with dimethylformamide (to separate the PSU homopolymer) and formic acid (to separate the PAI homopolymer). The residual material was dissolved in NMP and reprecipitated from water. After filtration and drying the powder was again extracted with dimethylformamide and formic acid. After these extractions the product was washed thoroughly with water and dried under vacuum at 130 °C for 24 h. The yield of PSU-PAI was 29%. Further details concerning the synthesis shall not be topic of this paper and can be obtained elsewhere.⁶ The structure is given in scheme 1: $M_n = 1.5 \times 10^4$; $M_w = 5.3 \times 10^4$; $T_g = 118$ °C (PAI); 189 °C (PSU); the composition of the block copolymer is PSU/PAI, 48 wt %/52 wt %.

Sample Preparation. (a) As-Cast Sample. A 5 wt % solution of the polymer in hexafluoroisopropanol (HFIP) was prepared. The solvent was removed in a high vacuum oven at 70 °C for 1 week. The thus obtained transparent films, having a thickness of about 1 mm, were then ultramicrotomed at room temperature using a diamond knife.

(b) Melt-Pressed Sample. About 0.5 g of the polymer was melt-pressed at 150 °C into a film specimen having a thickness of about 1 mm with a pressure of 100 kg/cm² for about 2 min.

Transmission Electron Microscopy. TEM, ESI, and electron energy loss spectroscopy (EELS) were carried out with a JEOL 2000FX equipped with a

[†] Kyoto University.

[‡] BASF AG.

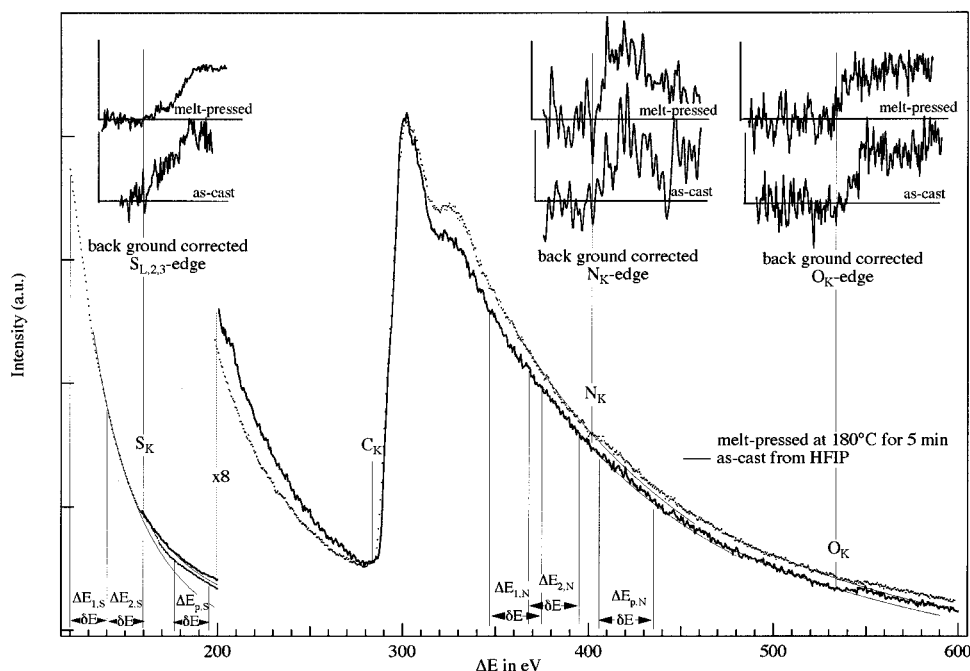
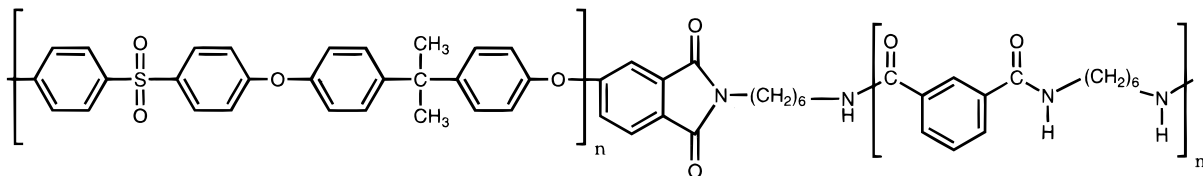


Figure 1. Electron energy loss spectra of the as-cast (solid line) and melt-pressed (dotted line) samples in the core-loss region from 150 to 600 eV, including the sulfur $L_{2,3}$ -edge ($S_{L_{2,3}}$) at $\Delta E = -165$ eV, carbon K-edge (C_K) at $\Delta E = -284$ eV, nitrogen K-edge (N_K) at $\Delta E = -401$ eV, and oxygen K-edge (O_K) at $\Delta E = -532$ eV. The sulfur and nitrogen edges were used for the determination of the element distribution images. Further the locations of the background and postedge images for the determination of the sulfur and nitrogen distributions are illustrated. The insets on top are the sulfur, nitrogen, and oxygen edges after subtracting the extrapolated background.

Scheme 1



GATAN 678 parallel electron energy loss spectrometer and imaging system. The acceleration voltage was $E_0 = 200$ keV and the collection angle $\delta = 6.79$ mrad. Element distribution images were acquired via the three-window method. To determine the sulfur distribution the $L_{2,3}$ edge at $\Delta E = -165$ eV was used. The background (preedge) images were taken at $\Delta E_{1,S} = -130$ eV and $\Delta E_{2,S} = -150$ eV, and the postedge image was at $\Delta E_{p,S} = -185$ eV with a energy width δE of 20 eV (see Figure 1). In the case of the nitrogen distribution the K-edge at $\Delta E = -401$ eV was used. The background images were taken at $\Delta E_{1,N} = -361$ eV and $\Delta E_{2,N} = -381$ eV, and the postedge image at $\Delta E_{p,N} = -421$ eV with an energy width δE of 30 eV (see Figure 1). In all cases the recording time for one respective image was 10 s.

Results and Discussion. Figure 1 shows the electron energy loss spectra of the as-cast (solid line) and melt-pressed (dotted line) samples. In order to sharpen the signal, background subtraction and Fourier-ratio deconvolution⁴ were applied. The spectra represent the elements extended over a circular area with about a 500 nm diameter. Since the domain spacing is about 30 nm (see later), the spectra show the absorption edges of elements contained in both the PSU (i.e., sulfone, $\Delta E_{L_{2,3}} = -165$ eV; carbon, $\Delta E_K = -284$ eV; oxygen, $\Delta E_K = -532$ eV) and the PA (i.e., nitrogen, $\Delta E_K = -401$ eV; carbon, $\Delta E_K = -284$ eV; oxygen, $\Delta E_K = -532$ eV). The difference in the elemental composition was now used

to determine the structure via element mapping. The images used to calculate the element distribution images with the three-window method will be presented elsewhere.⁷

Figure 2 shows the sulfur (a) and nitrogen (d) distribution images of the as-cast sample as obtained after the three-window method. In order to remove high-frequency noise two-dimensional Fourier transformation was applied to extract the structure information. Parts b and e of Figure 2 show the power spectra of the element distribution images. The Fourier modes with the highest intensity, i.e., the ring pattern in the center, corresponding to the signal caused by the phase-separated structures of the block copolymer with a characteristic spacing of about 30 nm, were extracted by masking the spectrum with a circular shaped mask shown by black color in the center of the figure. Note that the spectrum is circularly shaped, meaning that the structures have no preferential direction as expected from an as-cast film. After inverse Fourier transformation we obtain the more or less noise free element distribution images seen in Figure 2c,f. In the case of Figure 2c the bright area corresponds to a high sulfur content or the PSU phase, while in the case of Figure 2f the bright area corresponds to a high nitrogen content or the PA phase.

The sulfur (Figure 3a) and nitrogen (Figure 3b) distribution images of the melt-pressed sample were obtained in the same way as described in the previous

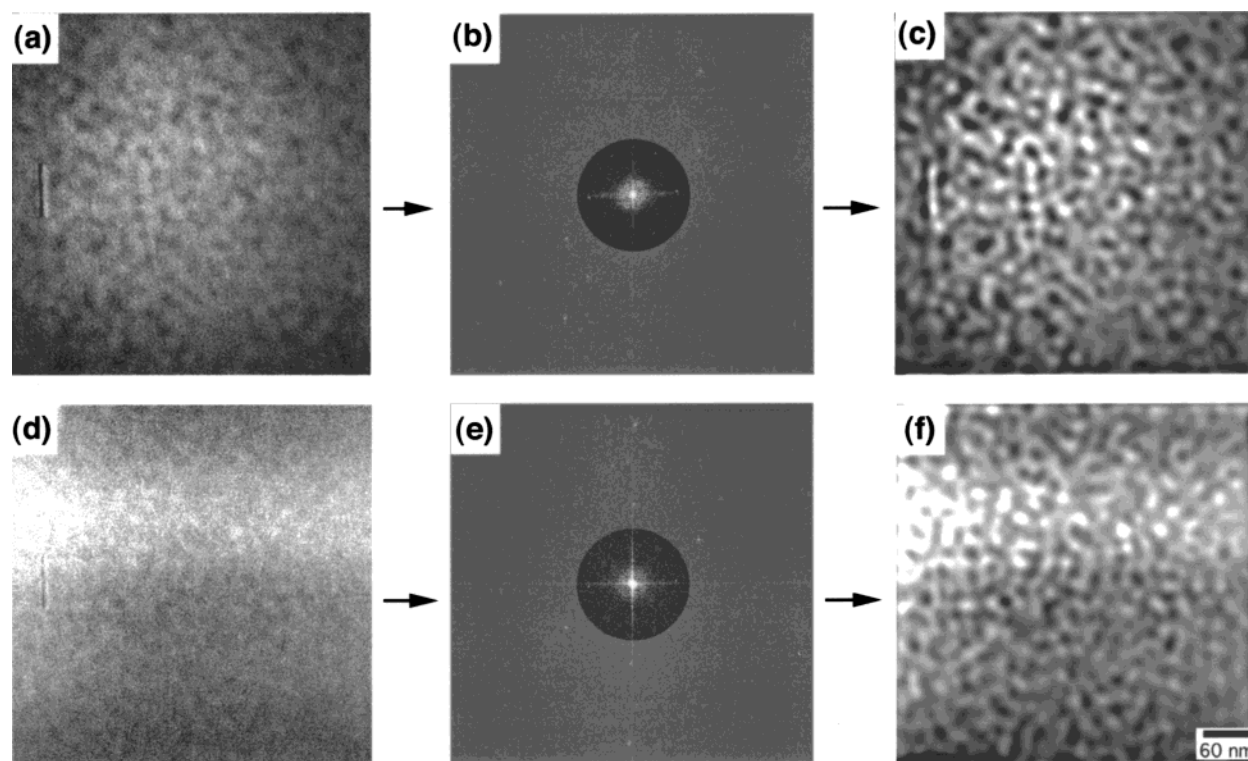


Figure 2. Sulfur (a) and nitrogen (d) distribution images of the as-cast sample as obtained from the three-window method. Parts b and c are the Fourier spectra of parts a and b, and the inverse Fourier transformations after applying a mask filter are given in parts c and f, respectively. The mask filter screens out all the Fourier modes outside the mask appearing in black circles.

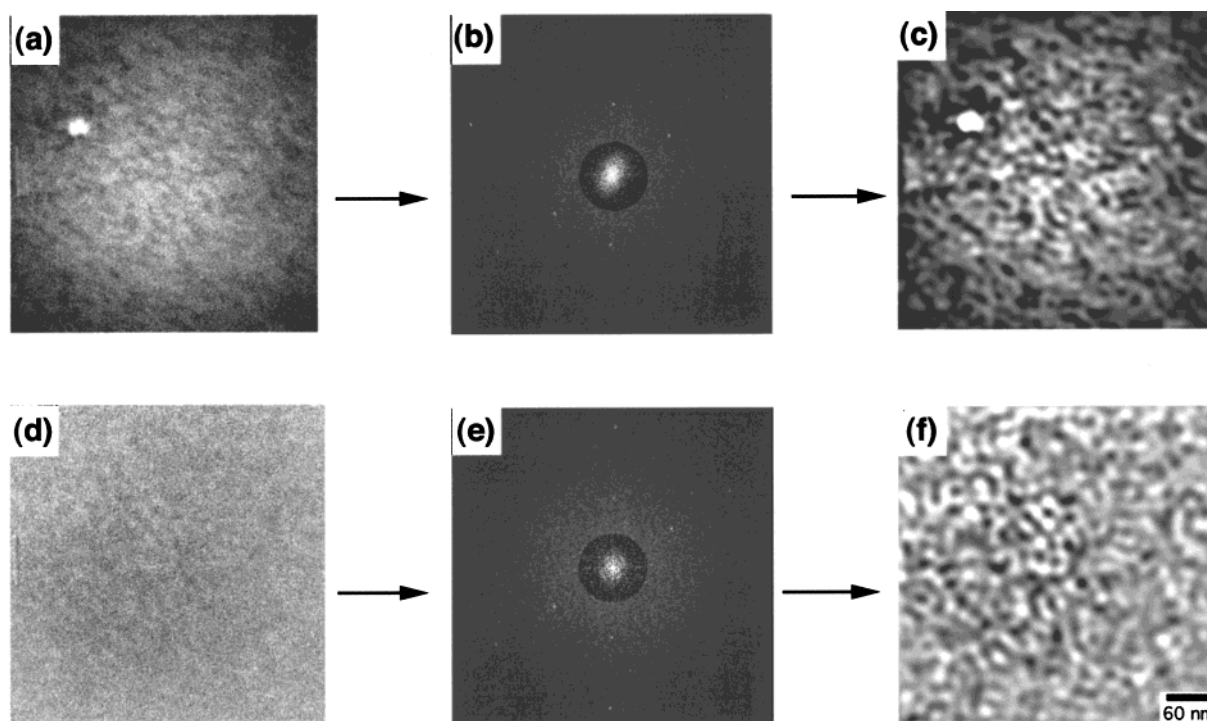


Figure 3. Sulfur (a) and nitrogen (d) distribution images of the melt-pressed sample as obtained from the three-window method. Parts b and c are the Fourier spectra of parts a and b and the inverse Fourier transformations after applying a mask filter are given in parts c and f, respectively. The mask filter screens out all the Fourier modes outside the mask appearing in black circles.

paragraph. In the case of the melt-pressed sample the Fourier spectrum is not circular, as can be seen in Figure 3b,e. The distortion of the spectrum is probably caused by a deformation of the phase-separated structure during the melt press process. After inverse Fourier transformation we obtain the noise-reduced sulfur (Figure 3c) and nitrogen (Figure 3f) distribution images.

Again the bright areas correspond to a high content of the respective element. Carefully looking at the images, one can see that the structure is actually distorted in one direction as indicated in the Fourier spectra.

In both the as-cast and melt-pressed samples, the average domain spacing is about 30 nm. This spacing is consistent with the spacing estimated from the SAXS

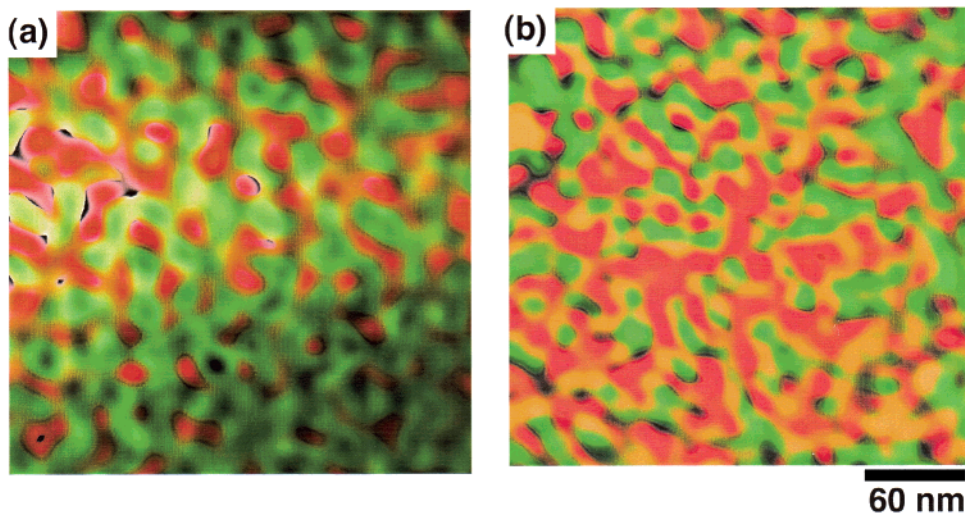


Figure 4. Comparison of the sulfur and nitrogen distribution images of the as-cast (a) and melt-pressed (b) samples. The images are complementary: the sulfur-containing phase (the PSU phase) is shown by a reddish color and the nitrogen-containing phase (the PA phase) by a greenish color.

profiles, which show a broad maximum or shoulder.⁷ In order to prove the reliability of the images, the complementarity of the sulfur and nitrogen images was checked. Figure 4 shows the overlay of the sulfur and nitrogen distribution images of the as-cast (a) and melt-pressed (b) samples. For better visualization the sulfur-containing phase was represented by a reddish (PSU) and the nitrogen-containing phase (PA) by a greenish color. This was achieved by reverting the original gray scale images to rgb (red-green-blue) scale images, selecting only the red (in the case of the PSU distribution) or green channel (in the case of the PA distribution) of the images, so the former bright area is transformed into a colored one. As one can clearly see, the structure obtained from the two independent measurements are complementary. In the interface region the sulfur and nitrogen distributions overlap, as visible from the yellow color generated by the overlay of the red color of the sulfur distribution and the green color of the nitrogen distribution. This overlap is generated by the curvature of the interface and the interface thickness of the PSU and PA in the ultrathin film. If the interface is not perpendicular to the film surface, there will be an overlapping part of the PSU and the PA along the depth of the film, and therefore sulfur and nitrogen will be detected at the same location. It is unlikely that the overlay is generated by mixing of the two phases as the PSU and PA are completely immiscible and will have a very small interfacial thickness, as we discussed in previous papers⁸ when investigating a blend of the same polymers. The samples presented here have a thickness of about 30 nm, which was also distinguished by EEL spectroscopy. The thickness is about equal to the observed average domain spacing, so that artifacts on the element distribution images due to overlapping of multiple phases in the thin film can be essentially neglected. A detailed description will be part of a forthcoming full paper.⁷ We are aware that the applied complex image processing is generating artifacts especially in the area close to the edge of the image caused

by the circular intensity distribution of the electron beam, the image processing steps, and the subsequent two-dimensional Fourier analysis, so one cannot expect to obtain quantitative perfectly matching nitrogen and sulfur distributions. The element distributions, however, are certainly sufficiently precise enough to allow a determination of the morphology at least qualitatively.

A unique morphology developed in the novel block copolymer PSU-PAI, for which the scattering methods unfortunately provide no specific information concerning the real space morphology, was visualized for the first time by using EFTEM. We conclude that the polydisperse PSU-PA shows features of a random bicontinuous spongelike morphology, meaning that the wide molecular weight distribution does not allow a highly ordered morphology as observed in almost monodisperse block copolymers.

References and Notes

- (1) Hunt, J. A.; Disko, M. M.; Behal, S. K.; Leapman, R.D. *Ultramicroscopy* **1995**, 58 (1), 55.
- (2) (a) Kunz, M.; Moeller, M.; Cantow H.-J. *Makromol. Chem., Rapid Commun.* **1987**, 8 (8), 401. (b) Eisenbach, C. D.; Ribbe, A.; Guenther, C. *Macromol. Rapid. Commun.* **1994**, 15, 395.
- (3) Ribbe, A.; Eisenbach, C. D. *Kautsch. Gummi Kunstst.* **1994**, 47 (10), 727.
- (4) Egerton, R. F. *Electron Energy Loss Spectroscopy in the Transmission Electron Microscope*; Plenum Press: New York, 1996.
- (5) (a) Matsuo, M.; Ueno, T.; Horino, H.; Chujyo S.; Asai, H. *Polymer* **1968**, 9, 425. (b) Inoue, T.; Soen, T.; Kawai, H.; Fukatsu, M.; Kurata, M. *J. Polym. Sci. Lett. Ed.* **1968**, 6, 75. (c) Inoue, T.; Soen, T.; Hashimoto, T.; Kawai, H. *J. Polym. Sci.* **1969**, 7, 1283.
- (6) Weber, M. Personal communications.
- (7) Ribbe, A.; Hayashi, M.; Weber, M.; Hashimoto, T. Manuscript in preparation.
- (8) (a) Hayashi, M.; Ribbe, A.; Weber, M.; Heckmann, W.; Hashimoto, T. *Polymer* **1997**, 39, 299–308. (b) Ribbe, A. E.; Hayashi, M.; Weber, M.; Hashimoto, T. *Polym. Commun.* **1998**, 39, 7149.

MA990533W